 CMES, vol.93, no.6, pp.411-440, 2013

Parameter Sensitivity and Probabilistic Analysis of the Elastic Homogenized Properties for Rubber Filled Polymers

Marcin Kamiński[1,2], **Bernd Lauke**[2]

Abstract: The main aim in this paper is a computational study devoted to the sensitivity gradients and probabilistic moments of the effective elastic parameters for the rubber-filled polymers. The methodology is based on least squares recovery of the polynomial functions relating the effective tensor components and the given input design/random parameters. All numerical experiments are provided with respect to Young's moduli of the elastomer constituents. Computational analysis is possible thanks to the application of the Response Function Method, which is enriched in our approach with the weighting procedures implemented according to the Dirac-type distributions. The homogenized elasticity tensor components are derived with the use of the variational upper and lower bounds for 2 D idealization of the composite and also thanks to the computational solution to the plane strain cell problem solved on the elastomer's Representative Volume Element. Sensitivity analysis results in the first order gradients of the effective tensor, while probabilistic moments consist of up to the fourth order probabilistic moments and coefficients of the tensor; all numerical experiments are carried out in the FEM-oriented code MCCEFF and also using the symbolic computer algebra system MAPLE. This approach is straightforwardly applicable in deterministic and probabilistic optimization of polymers filled with rubber or carbon particles; it gives also the basis to further homogenization-based experiments with more advanced constitutive laws like Mullins theory.

Keywords: homogenization method; sensitivity analysis; Finite Element Method; probabilistic analysis; least squares method; effective tensor upper and lower bounds.

[1] Department of Structural Mechanics, Faculty of Civil Engineering, Architecture and Environmental Engineering, Technical University of Lódź, Al. Politechniki 6, 90-924 Lódź, Poland. Tel: 48-42-6313571 Email: Marcin.Kaminski@p.lodz.pl

[2] Leibniz-Institut für Polymerforschung Dresden e.V., Hohe Strasse 6, 01069 Dresden, Germany. Email: laukeb@ipfdd.de

1 Introduction

It is widely known that polymers filled with rubber particles have random internal micro- and nanostructures [Jeulin and Ostoja-Starzewski (2001)], so that their mechanical modeling with the use of a homogenization procedure is well justified. We introduced here an effective medium with iso- or orthotropic character fulfilling some equivalence criteria [Christensen (1979); Milton (2002), Kamiński (2005)] instead of the real hierarchical heterogeneous structure with various levels and different types of an uncertainty. These criteria are developed starting from a simple spatial averaging of the RVE through some algebraic approximations for the upper and lower bounds as well as using the Finite Element Method solution to the so-called cell problem. The basic difference to the previous numerical experiments and theories with homogenization is that now the rubber particle embedded into the polymeric matrix has Young's modulus the few times smaller and, effectively, elasticity tensor components. The rubber particles in this context do not form a reinforcement to the matrix, but rather some kind of a filler (in the framework of elastic range by only). Nevertheless, prediction of the homogenized characteristics as well as their sensitivity gradients with respect to material parameters of the initial components and/or their probabilistic moments coming from a randomness in original materials characteristics is an important and challenging problem [Kamiński (2013); Kamiński and Lauke (2012); Ma et al. (2011)]. A solution to that issue would allow for a more optimal choice of the components for the specific applications of rubber-filled polymers as well as the homogenization-based reliability and durability predictions for such materials and structures. Let us note that alternatively to the homogenization method, one may employ the Voronoi Cell Finite Element Method (VCFEM) to provide direct micromechanical numerical modeling of the composites or porous materials as well [Dong and Atluri (2012)] and this alternative could be considered in the nearest future for further stochastic developments.

The main aim of this work is to contrast various homogenization methods for rubber-filled polymers in terms of sensitivity and randomness of the elastic characteristics of their constituents. Computational symbolic algebra plays a dominant role because we employed analytical and semi-analytical methods to accomplish this goal. Sensitivity analysis performed for the Young's moduli of both components and the filler's particles volume ratio enables to determine the most decisive design parameters for the different homogenization methods included in this comparison. Semi-analytical technique is based on the Least Squares Method (LSM) recovery of the response functions relating the homogenized tensor components with design/random input parameters. It is introduced using the deterministic Finite Element Method (FEM) experiments carried out using the homogenization-

oriented 4-noded plane strain element of the system MCCEFF (Monte-Carlo Constants EFFective) and based on the effective modules method [Kamiński (2005); Kamiński (2009); Kamiński (2013)]. The sets of such experiments' results are transferred thanks to the usage of the weighted version of the LSM into the response functions and, further, into the additional probabilistic moments calculated via the generalized stochastic perturbation technique. This technique has been chosen as the very fast and accurate, which was proved before by the comparative tests with the Monte-Carlo simulation technique [Kamiński and Lauke (2012)]. It is remarkable that this methodology may be used at the same time to determine both sensitivity gradients and probabilistic moments of the homogenized tensor in the presence of some input design/random variables. The Dirac distribution of the weights in the neighborhood of a mean value of the input parameter is preferred since the expectation of the chosen input parameter significantly prevails; it follows also previous computational experiments with polymeric composites with the reinforcing fibers. The response functions were assumed here in the polynomial form, so that it could be verified in the MAPLE experiments how an order of the given polynomial influences the expectations, coefficients of variation, skewness and kurtosis of the homogenized tensor components. Finally, the dependence of probabilistic moments and coefficients of this tensor on the initial uncertainty sources was verified quantitatively and it was checked additionally whether the homogenization method preserves Gaussian distribution in-between input and output random quantities. The key novel aspect here is an application of the generalized stochastic perturbation technique in its Weighted Least Squares Method (WLSM) version, where Dirac weighting procedure guarantees and speeds up probabilistic convergence as satisfactory numerical stability of the results; contrary to the previous studies [Kamiński (2009)], we used consecutively 10^{th} order approximation for all the computed probabilistic moments and coefficients of the composite's effective properties.

2 Governing equations

2.1 Homogenization methods

Let us consider a plane cross-section of the particle-filled composite with linearly elastic and transversely isotropic properties of the components. The Representative Volume Element (RVE) Ω of Y ($Y \subset \Re^2$) as well as the section of this composite in the plane $x_3 = 0$ are shown in Fig. 1.

The region Ω contains two perfectly bonded, coherent and disjoint subsets Ω_1 (filler) and Ω_2 (matrix), and let the scale between corresponding geometrical diameters of Ω and Y be described by the small parameter $\varepsilon > 0$. The parameter ε

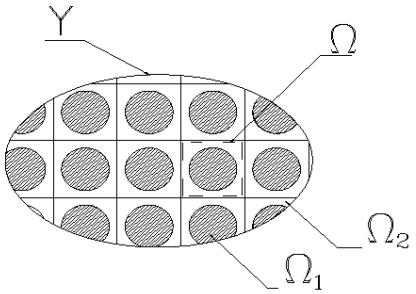

Figure 1: Periodic two-component composite idealization

indexes all the tensors written for the geometrical scale of Ω, and let $\partial\Omega$ denote the external boundary of Ω, while $\partial\Omega_{12}$ is the interface boundary between the Ω_1 and Ω_2 regions. Further, it is assumed that the composite is periodic in a random sense if, for an additional ω belonging to a suitable probability space – there exists some specific geometrical transformation in-between Ω and the entire composite Y. Next, let us introduce two different coordinate systems: $\mathbf{y} = (y_1, y_2)$ at the micro scale of the composite and $\mathbf{x} = (x_1, x_2)$ at the macro-scale. A periodic state function F was defined in the region Y:

$$F^{\varepsilon}(\mathbf{x}) = F\left(\frac{\mathbf{x}}{\varepsilon}\right) = F(\mathbf{y}). \tag{1}$$

This expression makes it possible to describe the macro functions (connected with the macro-scale of a composite) in terms of micro ones and vice versa. The elasticity coefficients can be defined, for instance, as

$$C^{\varepsilon}_{ijkl}(\mathbf{x}) = C_{ijkl}(\mathbf{y}). \tag{2}$$

fulfilling the symmetry, boundedness and ellipticity conditions. Moreover, for any of the composite constituents, this tensor is defined as

$$C_{ijkl}(\mathbf{x}) = E(\mathbf{x}) \left\{ \delta_{ij}\delta_{kl} \frac{\nu(\mathbf{x})}{(1+\nu(\mathbf{x}))(1-2\nu(\mathbf{x}))} + (\delta_{ik}\delta_{jl} + \delta_{il}\delta_{jk}) \frac{1}{2(1+\nu(\mathbf{x}))} \right\}. \tag{3}$$

Because we introduce

$$A_{ijkl}(x) = \delta_{ij}\delta_{kl} \frac{\nu(x)}{(1+\nu(x))(1-2\nu(x))} + (\delta_{ik}\delta_{jl} + \delta_{il}\delta_{jk}) \frac{1}{2(1+\nu(x))} \tag{4}$$

then the first partial derivatives of the elasticity tensor with respect to the Young's modulus in the homogeneous material are equal to

$$\frac{\partial C_{ijkl}}{\partial e} = A_{ijkl}, \tag{5}$$

and any higher order partial derivatives are equal to 0. Further, the effective tensor $C_{ijkl}^{(eff)}$ is introduced as a tensor that replaces C_{ijkl}^{ε} with $C_{ijkl}^{(eff)}$ in the following equilibrium equations:

$$\left(C_{ijkl}^{\varepsilon}\, \varepsilon_{kl}\left(\mathbf{u}^{\varepsilon}\right)\right)_{,j} = 0; \quad \mathbf{x} \in \Omega \tag{6}$$

$$\varepsilon_{ij}\left(\mathbf{u}^{\varepsilon}\right) \;=\; \tfrac{1}{2}\left(u_{i,j}^{\varepsilon} + u_{j,i}^{\varepsilon}\right);\, \mathbf{x} \in \Omega \tag{7}$$

$$C_{ijkl}^{\varepsilon}(\mathbf{x}) \;=\; \chi_1(\mathbf{x}) C_{ijkl}^{(1)} + (1 - \chi_1(\mathbf{x}))\, C_{ijkl}^{(2)} \tag{8}$$

with $\mathbf{u}^{\varepsilon}$ as displacements, where $\mathbf{u}^0$ is obtained as a solution for a weak limit of $\mathbf{u}^{\varepsilon}$ with $\varepsilon \to 0$. The tensors $C_{ijkl}^{(eff)}$ and $C_{ijkl}^{(eff)}$ are the elasticity tensor components of the fiber filler or particle and the matrix, respectively, while the characteristic function appearing in the above equation is defined as

$$\psi_1(\mathbf{x}) = \begin{cases} 1, & x \in \Omega_1 \\ 0, & x \in \Omega_2 \end{cases}, \tag{9}$$

with the following displacements boundary conditions on all the external edges of the RVE

$$\mathbf{u}^{\varepsilon} = 0;\, \mathbf{x} \in \partial\Omega_u \equiv \partial\Omega \tag{10}$$

and these corresponding to the stresses given at the fiber-matrix interface

$$\sigma_{ij} n_j = p_i; \quad \mathbf{x} \in \partial\Omega_\sigma \equiv \partial\Omega_{12} \tag{11}$$

The homogenization problem is to find the limit of the solution $\mathbf{u}^{\varepsilon}$ with ε tending to zero [Bensoussan et al. (1979); Sanchez-Palencia (1980); Fish and Chen (2001)]. A variational statement equivalent to the equilibrium problem (6-10) is to find a displacement $\mathbf{u}^{\varepsilon}$ fulfilling the following equation:

$$\int_{\Omega} C_{ijkl}\left(\tfrac{\mathbf{x}}{\varepsilon}\right)\; \varepsilon_{ij}(\mathbf{u})\, \varepsilon_{kl}(\mathbf{v})\, d\Omega = \int_{\partial\Omega_\sigma} p_i v_i d\left(\partial\Omega\right), \tag{12}$$

where vector function $\mathbf{v}$ (or v_i, i=1,2) in the above relation is any admissible vector displacement function fulfilling the boundary conditions given in Eqn. (11). The

limiting solution is called further homogenization function $\chi_{(pq)}$ (p,q=1,2) - a solution to the local problem (6-10), where the following stress boundary conditions are applied at the interface [Kamiński (2005)]:

$$\sigma_{ij}\left(c_{(pq)}\right)n_j = [C_{ijpq}]\,n_j = F_{(pq)i}\ ; \quad \mathbf{x} \in \partial\Omega_{12}, \tag{13}$$

and where n_j is the component of the unit vector normal to the particle-matrix boundary directed to the particle interior; $[C_{ijpq}]$ denotes the difference of the elasticity tensor for the matrix and the particle

$$[C_{ijpq}] = C^{(m)}_{ijpq} - C^{(p)}_{ijpq}. \tag{14}$$

The stress boundary conditions corresponding to different homogenization problems are specified in Tab. 1 for three independent homogenization functions.

Table 1: The components of the interface forces $F_{(pq)i}$

	$\chi_{(11)}$	$\chi_{(12)}$	$\chi_{(22)}$
$F_{(pq)1}$	$C^{(2)}_{1111} - C^{(1)}_{1111}$	$C^{(2)}_{1212} - C^{(1)}_{1212}$	$C^{(2)}_{1122} - C^{(1)}_{1122}$
$F_{(pq)2}$	$C^{(2)}_{2211} - C^{(1)}_{2211}$	$C^{(2)}_{1212} - C^{(1)}_{1212}$	$C^{(2)}_{2222} - C^{(1)}_{2222}$

Then, an equivalent homogeneous orthotropic elastic material is obtained, characterized by the tensor

$$C^{(eff)}_{ijkl} = \frac{1}{|\Omega|}\int_{\Omega}\left(C_{ijkl} + C_{ijmn}\varepsilon_{mn}\left(\chi_{(kl)}\right)\right)d\Omega. \tag{15}$$

From the engineering point of view the most interesting issue is the effectiveness of such a characterization of $C^{(eff)}_{ijkl}$, which can be approximated as the difference between upper and lower estimates and, on the other hand, sensitivity of the effective tensor with respect to material characteristics of the constituents. It can be proved that there exist such tensors $\inf\left(C_{ijkl}\right)$ and $\sup\left(C_{ijkl}\right)$ [Christensen (1979)] that

$$\inf\left(C_{ijkl}\right) \le C^{(eff)}_{ijkl} \le \sup\left(C_{ijkl}\right) \tag{16}$$

It is well known that the theorem of minimum potential energy gives the upper bounds of the effective tensor, whereas the minimum complementary energy ap-

proximates the lower bounds. Thanks to the Eshelby's formula, the explicit equations for the bulk κ and shear moduli μ are given as follows:

$$\begin{cases} \sup \kappa = \left[\sum_{r=1}^{N} \mathrm{v}_r \left(\kappa_u + \kappa_r \right)^{-1} \right]^{-1} - \kappa_u \\ \sup \mu = \left[\sum_{r=1}^{N} \mathrm{v}_r \left(\mu_u + \mu_r \right)^{-1} \right]^{-1} - \mu_u \end{cases} \tag{17}$$

where κ_u, μ_u have the following form:

$$\begin{cases} \kappa_u = \frac{4}{3} \mu_{\max} \\ \mu_u = \frac{3}{2} \left(\frac{1}{\mu_{\max}} + \frac{10}{9\kappa_{\max} + 8\mu_{\max}} \right)^{-1} \end{cases} \tag{18}$$

N stands here for a total number of composite constituents, where v_r, $1 \leq r \leq N$ denote their volume fractions. Further, lower bounds for the elasticity tensor are obtained as

$$\begin{cases} \inf \kappa = \left[\sum_{r=1}^{N} \mathrm{v}_r \left(\kappa_l + \kappa_r \right)^{-1} \right]^{-1} - \kappa_l \\ \inf \mu = \left[\sum_{r=1}^{N} \mathrm{v}_r \left(\mu_l + \mu_r \right)^{-1} \right]^{-1} - \mu_l \end{cases} \tag{19}$$

where it holds that

$$\begin{cases} \kappa_l = \frac{4}{3} \mu_{\min} \\ \mu_l = \frac{3}{2} \left(\frac{1}{\mu_{\min}} + \frac{10}{9\kappa_{\min} + 8\mu_{\min}} \right)^{-1} \end{cases} \tag{20}$$

It should be noted that

$$\kappa_l = \frac{E_l}{3\left(1 - 2\upsilon_l\right)}, \quad \mu_l = \frac{E_l}{2\left(1 + \upsilon_l\right)}, \quad \lambda_l = \kappa_l - \tfrac{2}{3}\mu_l \tag{21}$$

$$C^{(l)}_{\alpha\beta\gamma\delta} = \delta_{\alpha\beta}\delta_{\gamma\delta}\lambda_l + \left(\delta_{\alpha\gamma}\delta_{\beta\delta} + \delta_{\alpha\delta}\delta_{\beta\gamma}\right)\mu_l \tag{22}$$

where E_l is lower bound on the Young's modulus and ν_l is the same bound on the Poisson's ratio.

Finally, let us define two fundamental problems P_1 and P_2, whose solution was provided here [Kamiński (2009)]:

P_1 : Find $\frac{\partial^\alpha C^{(eff)}_{ijkl}}{\partial \mathbf{h}^\alpha}$ for $\alpha \in \mathrm{N}$, where $\mathbf{h} = \mathbf{h}(\mathbf{x}) = \{E_1, E_2\}$, where

$$\mathbf{h}(\mathbf{x}) = \chi_1(\mathbf{x})\, h_1 + (1 - \chi_1(\mathbf{x}))\, h_2. \tag{23}$$

P_2: Find $\mu_\alpha\left(C_{ijkl}^{(eff)}\right)$ where $\alpha \in \mathrm{N}$, $\mathbf{b}(\mathbf{x};\omega) = \{E_1(\omega), E_2(\omega)\}$, where

$$\mu_\alpha(\mathbf{b}(\mathbf{x};\omega)) = \psi_1(\mathbf{x})\,\mu_\alpha(b_1(\omega)) + (1-\psi_1(\mathbf{x}))\,\mu_\alpha(b_2(\omega)). \tag{24}$$

with $\mu_\alpha(\mathbf{b}(\mathbf{x};\omega))$ being αth order central probabilistic moment of $\mathbf{b}(\mathbf{x};\omega)$ and ψ_1 from Eqn (9).

2.2 Stochastic generalized perturbation method in homogenization

To provide the stochastic perturbation technique based on the Taylor series expansion we denote the random vector of the problem as $\boldsymbol{b}(\omega)$ and we assume that it has M components, so that mth order central probabilistic moment is obviously given by

$$Cov(b^r, b^s) = \int_{-\infty}^{+\infty}\int_{-\infty}^{+\infty} (b^r - E[b^r])(b^s - E[b^s])g(b^r, b^s)db^r db^s, \quad r,s = 1,...,M \tag{25}$$

with $g(b^r, b^s)$ as the probability density function (PDF) of the component b_p. According to the main philosophy of this method, all functions in the basic deterministic problem (heat conductivity, heat capacity, temperature and its gradient as well as the material density) are expressed similarly to the following finite expansion of a random tensor function $C_{ijkl}^{(eff)}$ [Kamiński (2013)]:

$$f\left(C_{ijkl}^{(eff)}\right) = f^0\left(C_{ijkl}^{(eff)0}\right) + \theta\left.\frac{\partial C_{ijkl}^{(eff)}}{\partial b}\right|_{b=b^0}\Delta b + ... + \frac{\theta^n}{n!}\left.\frac{\partial^n C_{ijkl}^{(eff)}}{\partial b^n}\right|_{b=b^0}\Delta b^n, \tag{26}$$

where θ is a given perturbation parameter (taken usually as equal to 1), while the nth order variation is given as follows:

$$\theta^n \Delta b^n = (\delta b)^n = \varepsilon^n\left(b - b^0\right)^n. \tag{27}$$

We postpone for a simplicity in all further equations notation the fact that all partial derivatives are determined at the expectation of the input random variable (provided formerly only in Eqn. (26)). The expected values for $C_{ijkl}^{(eff)}$ are exactly given using the 10^{th} order expansion as [Kamiński (2013)]

$$E\left[C_{ijkl}^{(eff)}\right] = f^0\left(C_{ijkl}^{(eff)0}\right) + \sum_{p=1}^{M}\frac{\theta^2}{2}\frac{\partial^2 C_{ijkl}^{(eff)}}{\partial b_p^2}\mu_2(b_p) + \sum_{p=1}^{M}\frac{\theta^4}{4!}\frac{\partial^4 C_{ijkl}^{(eff)}}{\partial b_p^4}\mu_4(b_p) +$$
$$+ \sum_{p=1}^{M}\frac{\theta^6}{6!}\frac{\partial^6 C_{ijkl}^{(eff)}}{\partial b_p^6}\mu_6(b_p) + \sum_{p=1}^{M}\frac{\theta^8}{8!}\frac{\partial^8 C_{ijkl}^{(eff)}}{\partial b_p^8}\mu_8(b_p) + \sum_{p=1}^{M}\frac{\theta^{10}}{10!}\frac{\partial^{10} C_{ijkl}^{(eff)}}{\partial b_p^{10}}\mu_{10}(b_p)$$

(28)

where the central moments of the component p of random vector $\mathbf{b}$ may be obviously simply recovered here as

$$\mu_m(b_p) = \begin{cases} 0; & m = 2k+1 \\ \sigma^m(b_p)(m-1)!!; & m = 2k \end{cases} \tag{29}$$

for any natural $k \leq 1$with $\sigma^m(b_p)$ denoting mth power of the standard deviation for the variable b_p. Usually, according to some previous convergence studies, we may limit this expansion to the 10^{th} order and, consecutively, for all the moments of an interest here. Quite similar considerations lead to the expressions for higher moments, like the variance, third and fourth order central probabilistic moments (see Appendix). Finally, one may recover the coefficient of variation α, kurtosis γ and the skewness β from their well-known definitions as

$$\begin{aligned} \alpha\left(C_{ijkl}^{(eff)}\right) &= \sqrt{\frac{Var\left(C_{ijkl}^{(eff)}\right)}{E^2\left[C_{ijkl}^{(eff)}\right]}}, \quad \kappa\left(C_{ijkl}^{(eff)}\right) = \frac{\mu_4\left(C_{ijkl}^{(eff)}\right)}{\sigma^4\left(C_{ijkl}^{(eff)}\right)} - 3, \\ \beta\left(C_{ijkl}^{(eff)}\right) &= \frac{\mu_3\left(C_{ijkl}^{(eff)}\right)}{\sigma^3\left(C_{ijkl}^{(eff)}\right)}, \quad \alpha,\beta,\gamma,\delta = 1,2. \end{aligned} \tag{30}$$

Further, we provide a mathematical basis for the Least Squares Method (LSM) adjacent to the fourth order tensor in both non-weighted (NLSM) and weighted (WLSM) versions [Kamiński (2013)]. We use a polynomial approximation of the sth order (indexed by β here) through n numerical tests of the homogenization problem solved around the mean value of the given design parameter h; a result we obtain n different pairs $\left(h_\alpha, C_{ijkl}^{(eff)(\alpha)}\right)$ for α=1,...,n. We look for the following as polynomial approximation:

$$C_{ijkl}^{(eff)} \cong D_{ijkl}^{(\beta)} h^\beta = f\left(\mathbf{D}_{ijkl}, h\right) \quad \beta = 1,...,s;\ s < n;\ \ i,j,k,l = 1,2,3. \tag{31}$$

We introduce for this purpose the residuals in each trial point and each component of the homogenized tensor, i.e.

$$r_{ijkl(\alpha)} = C_{ijkl}^{(eff)(\alpha)} - f\left(\mathbf{D}_{ijkl}, h_\alpha\right) \quad \alpha = 1,...,n;\ \ i,j,k,l = 1,2,3. \tag{32}$$

Therefore, the goal is to determine the coefficients $\mathbf{D}_{ijkl}$ and it is done by a minimization of the weighted residuals functional provided as

$$S_{ijkl} = \sum_{\alpha=1}^{n} w_{\alpha\alpha} r_{ijkl(\alpha)}^2 \quad \alpha = 1,...,n;\ \ i,j,k,l = 1,2,3. \tag{33}$$

So that

$$\frac{\partial S_{ijkl}}{\partial D_{ijkl}^{(\beta)}} = -2\sum_{\alpha=1}^{n} w_{\alpha\alpha} r_{ijkl(\alpha)} \frac{\partial f\left(\mathbf{D}_{ijkl}, h_\alpha\right)}{\partial D_{ijkl}(\beta)} \quad \beta = 1,...,s; \quad i,j,k,l = 1,2,3. \tag{34}$$

Further, we adopt the following notation:

$$\mathbf{J}^{ijkl} = J_{\alpha\beta}^{ijkl} = \frac{\partial f\left(\mathbf{D}_{ijkl}, h_\alpha\right)}{\partial D_{ijkl}^{(\beta)}} \quad \alpha = 1,...,n; \quad \beta = 1,...,s; \quad i,j,k,l = 1,2,3. \tag{35}$$

and we form the modified equations as

$$\sum_{\alpha=1}^{n}\sum_{\beta=1}^{s} J_{\alpha\beta}^{ijkl} w_{\alpha\alpha} J_{\alpha\beta}^{ijkl} D_{ijkl}^{(\beta)} = \sum_{\alpha=1}^{n} J_{\alpha\beta}^{ijkl} w_{\alpha\alpha} C_{ijkl}^{(eff)(\alpha)}, \tag{36}$$
$$\alpha = 1,...,n;\ \beta = 1,...,s;\ i,j,k,l = 1,2,3.$$

obtaining the matrix normal equations

$$\left(\left(\mathbf{J}^{ijkl}\right)^T \mathbf{w}\, \mathbf{J}^{ijkl}\right) \mathbf{D}^{ijkl} = \left(\mathbf{J}^{ijkl}\right)^T \mathbf{w}\, \mathbf{C}_{ijkl}^{(eff)}, \quad i,j,k,l = 1,2,3. \tag{37}$$

This equations system (with the dimensions n x s) is solved symbolically in the system MAPLE for each component of the homogenized tensor separately to determine n coefficients of the polynomial expansion of the homogenized tensor with respect to the given h (multicomponent vector or a single variable). Obviously, we replace h with b in probabilistic analysis. After numerical solution to this equation, a final polynomial approximation is obtained and such a form of the approximating function is well justified by the numerical experiments performed in the next section. The main aim of the weighting procedure inserted into the least squares approximation for the homogenized tensor components with respect to the input design variable is to speed up the numerical convergence for the sensitivity coefficients of the homogenized tensor together with the polynomial order.

Algebraic determination of the response function – effective elasticity tensor components versus design parameters – enables, after simple normalization, to calculate sensitivity coefficients in the problem P_1. There holds

$$\begin{aligned}\frac{dC_{ijkl}^{(eff)}}{d\mathbf{h}} =& \frac{1}{|\Omega|}\int_{\Omega} \frac{\partial C_{ijkl}}{\partial \mathbf{h}} d\Omega + \frac{1}{|\Omega|}\int_{\Omega} \frac{\partial C_{ijmn}}{\partial \mathbf{h}} \varepsilon_{mn}\left(\chi_{(kl)}\right) d\Omega \\ &+ \frac{1}{|\Omega|}\int_{\Omega} C_{ijmn} \frac{\partial \varepsilon_{mn}\left(\chi_{(kl)}\right)}{\partial \mathbf{h}} d\Omega.\end{aligned} \tag{38}$$

Considering further computational efforts it is seen that the first component of the R.H.S. summation may be determined analytically, the second – via the combination of analytical differentiation with the additional FEM experiments, while the last one – with the use of semi-analytical method presented in this paper, for instance.

3 Numerical analysis

3.1 Deterministic analysis

We solve in this section the problem P_1 given by Eqn. (23) and the numerical analysis of the periodic particle composite homogenization is entirely performed for analytical formulas using symbolic analysis system MAPLE, v. 13. Elastic parameters of the rubber particle are taken as E_1=1.0 MPa, ν_1=0.4998, while for the polymer matrix E_2=4.0 GPa and ν_2=0.34 were used. The sensitivity gradients of various estimates for the homogenized tensor computed with respect to the Young's moduli of both components were compared as a simple spatial averaging method ('*Spatial averaging*') as well as two-dimensional upper and lower bounds ('*Lower bounds*' and '*Upper bounds*') on the homogenized tensor. The sensitivity gradients resulting from the analytical derivations are determined and presented with respect to the filler's volume fraction v_p and are collected in Figs. 3, 5, 7 with addition to $C_{1111}^{(eff)}$, $C_{1122}^{(eff)}$ and $C_{1212}^{(eff)}$, respectively. Sensitivity analysis based on the Response Function Method was performed using the same mean values of the elastic parameters and specifically for the filler volume ratio equal to 0.465. The homogenization oriented FEM program MCCEFF is employed and its internal automatic mesh generator is used to prepare a discretization with 144 quadrilateral 4-noded plane strain finite elements and 153 nodes – full periodicity cell with centrally located round filler (Fig. 2). We carried out 11 independent numerical tests for E_1 and E_2 separately, taking the following two sets of variability of these parameters: [0.5,0.6,0.7,0.8,0.9,1.0,1.1,1.2,1.3,1.4,1.5] MPa and [1.5,2.0,2.5,3.0,3.5,4.0,4.5,5.0,5.5,6.0,6.5] GPa. The gradients coming from this analysis are contrasted in Figs. 4, 6 and 8 to enable a direct comparison with Figs. 3, 5, 7, and further – in addition to the order of the polynomial response function marked on the horizontal axes. These gradients are computed using three various numerical schemes – in the ULSM (Unweighted Least Squares Method) (the weights distribution is [1,1,1,1,1,1,1,1,1,1,1]) as well as WLSM (its weighted version) methodologies consistent with triangular and Dirac distributions of the weights around the mean value of the design parameter (the sets [1,2,3,4,5,6,5,4,3, 2,1] and [1,1,1,1,1,6,1,1,1,1,1], correspondingly).

A general result obtained for all components of the homogenized tensor according

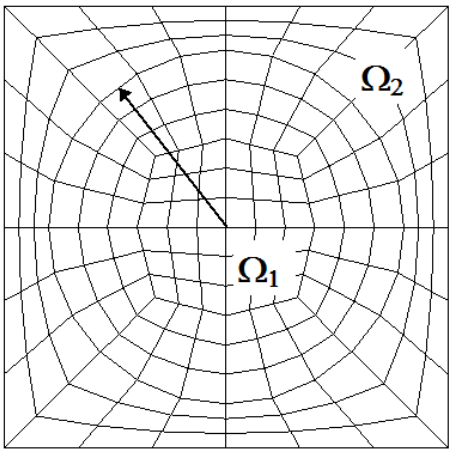

Figure 2: Finite Element Method discretization of the RVE

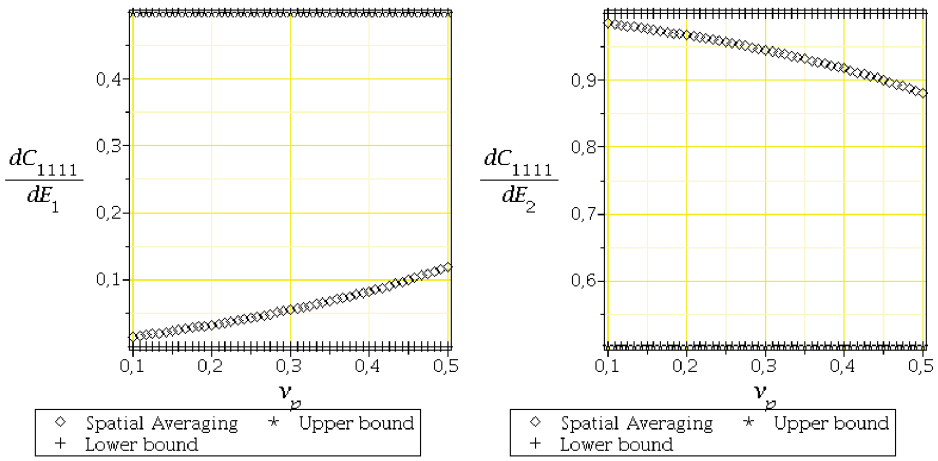

Figure 3: Sensitivity gradients of $C_{1111}^{(eff)}$ with respect to the particle (left) and matrix (right) Young's modulus

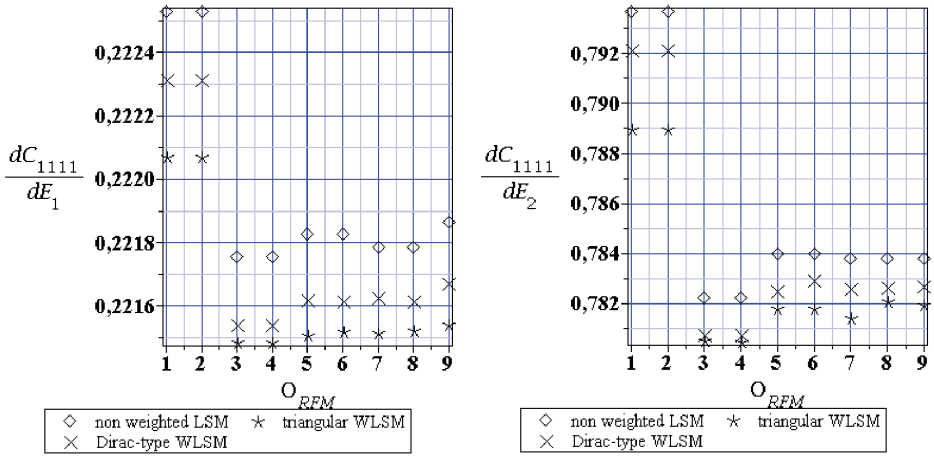

Figure 4: Response Function Method sensitivity gradients of $C_{1111}^{(eff)}$ with respect to the particle (left) and matrix (right) Young's modulus; LSM – Least Squares Method, WLSM – Weighted Least Squares Method

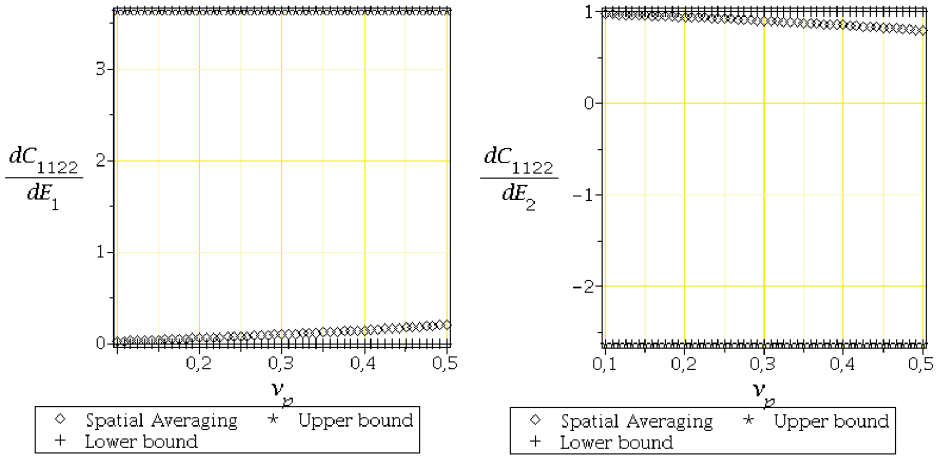

Figure 5: Sensitivity gradients of $C_{1122}^{(eff)}$ with respect to the particle (left) and matrix (right) Young's modulus

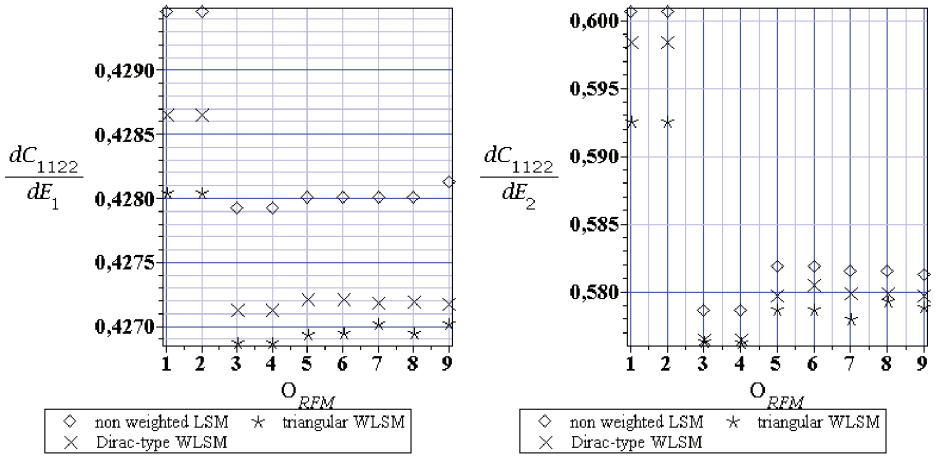

Figure 6: Response Function Method sensitivity gradients of $C_{1122}^{(eff)}$ with respect to the particle (left) and matrix (right) Young's modulus; LSM – Least Squares Method, WLSM – Weighted Least Squares Method

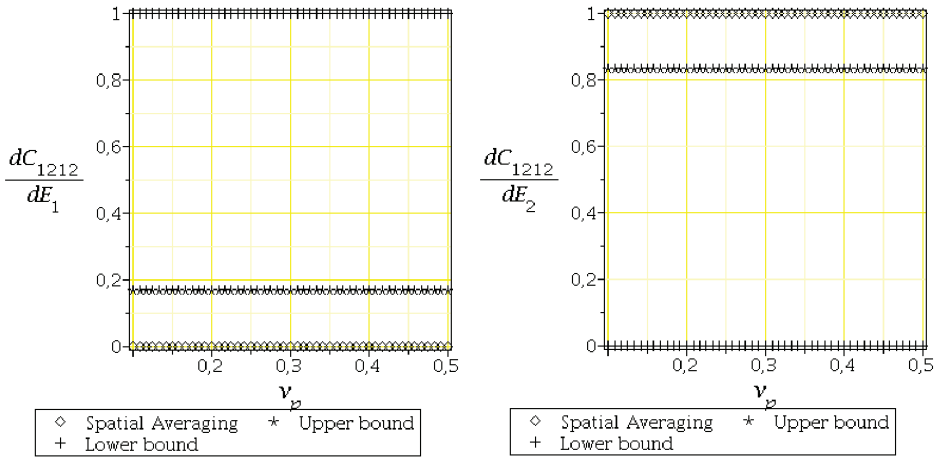

Figure 7: Sensitivity gradients of $C_{1212}^{(eff)}$ with respect to the particle (left) and matrix (right) Young's modulus

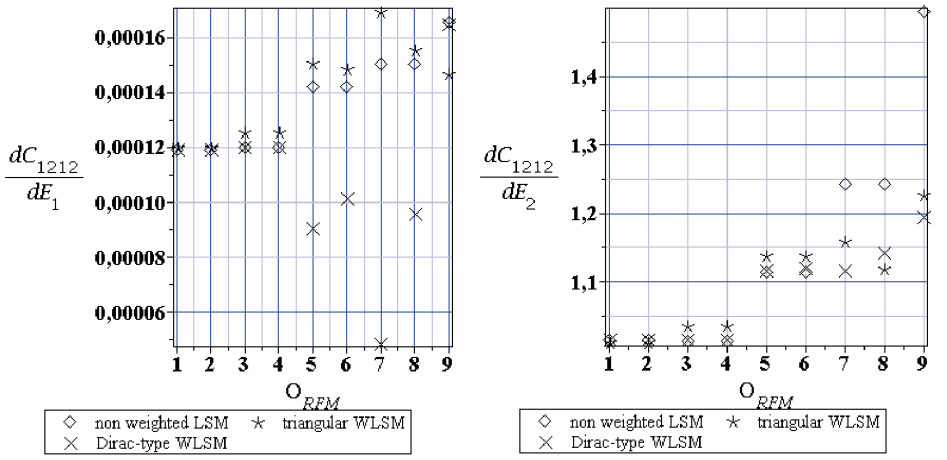

Figure 8: Response Function Method sensitivity gradients of $C_{1212}^{(eff)}$ with respect to the particle (left) and matrix (right) Young's modulus; LSM – Least Squares Method, WLSM – Weighted Least Squares Method

to all the methods is that all sensitivity gradients are positive with respect to both particle and matrix elastic moduli; the only exception is in case of upper bounds of $C_{1122}^{(eff)}$ determined with respect to E_2. This fact is independent of the filler ratio and of a determination way of this tensor. It means of course that the larger the elasticity moduli of both components, the larger the effective elasticity tensor components, which agree perfectly with an engineering intuition. Further, we notice that the gradients computed for the upper and lower bounds and quite insensitive to this filler ratio (considering additional algebraic equations), while spatial averages of the elasticity tensor shows positive sensitivity to E_1 and negative – to E_2, except once more $C_{1122}^{(eff)}$ – the larger the filler, the larger the influence on the homogenized tensor and the smaller the influence (and resulting gradient) of the matrix, which is confirmed by the right diagrams of Figs. 3 and 5. Absolute maximum results we compute for the gradients of $C_{1122}^{(eff)}$ determined with respect to E_1in case of the upper bounds of the elasticity tensor, while total minimum is noticed for the same component, while E_2 is the design input parameter in upper bounds' symbolic determination. However, the gradients of upper bounds not necessarily have greater values than these computed for the corresponding lower bounds - upper bounds return larger gradients for $C_{1111}^{(eff)}$ and $C_{1122}^{(eff)}$ with respect to E_1 and smaller sensitivity coefficients in case of E_2, while inverse relation is observed for $C_{1212}^{(eff)}$. The gradients of the averaged elastic tensor have intermediate values for the first components

of the elasticity tensor, whereas reach minimum and maximum, correspondingly, for $C_{1212}^{(eff)}$ while computed with respect to E_1 and E_2.

The gradients computed via the Response Function Method FEM experiments keep for the first two components two-side bounded by the corresponding gradients of the 2D upper and lower bounds for the effective tensor. As usually, the component $C_{1212}^{(eff)}$ is an exception, where smaller gradients than these corresponding to the bounds are noticed for E_1, while decisively larger – when E_2 is considered. We can notice moreover that for this specific volume ratio practically all the components' gradients of the homogenized tensor are significantly larger when computed with respect to E_2 than for the Young's modulus of the rubber filler. This observation has an engineering importance because Young's modulus of the matrix may be modified rather easily – by a proper design of the elastomer composition. The RFM-FEM technique appears to be the very efficient one from the computational point of view since practically no changes with respect to the RFM polynomial order are noticed in case of E_2 gradients; so that a type of the LSM has no matter for this part of numerical analysis. Slightly different situation is observed for the gradients with respect to E_1, where these differences are counted in the percents – in-between the lowest and the highest order (except the component $C_{1212}^{(eff)}$). The least numerical stability of the results is documented for the ULSM (unweighted) data series, while the best – for the Dirac distribution of the weights and this method is advised for further numerical experiments, with both sensitivity and probabilistic moments. The very interesting observation can be made from the gradients of the component $C_{1212}^{(eff)}$, where they seem to diverge together with the approximating polynomial order and this is due to the fact that practically both analyzed response functions to filler and matrix Young's modulus are of a linear nature, while higher order approximations bring some numerical inconsistencies only.

3.2 Probabilistic illustration

Probabilistic analysis focused on a solution to the problem P_2 formulated in Eqn. (25) was provided using a combination of the systems MCCEFF and MAPLE to compute up to the fourth order probabilistic moments and the coefficients of the effective elasticity tensor. Finite Element Method solution to the cell problem was carried out on the same mesh as in the previous section with the sensitivity analysis. The Young's moduli of the rubber and the matrix were defined as the input Gaussian random variables separately, because both Poisson's ratios demonstrate very small random dispersion in engineering practice. Moreover, Poisson's ratio of the rubber particle is almost equal to the upper physical limit of this parameter, so that its randomization according to one-sided and evidently non-Gaussian distribution is very challenging, quite separate computational issue (even with the Monte-Carlo simu-

lation scheme). Both input variables are represented using 11 points discrete sets (including expectation, as before in Sec. 4.1) and homogenized tensor components are identified from 11 independent FEM tests with varying Young's modulus. Input coefficients of variation (COV) of both Young's moduli are additional input parameters of this study and are taken from the interval [0.0,0.10] during computations of $C_{ijkl}^{(eff)}$ expectations, coefficients of variation, skewness and kurtosis, see Figs. 9-20 below. Considering previous numerical illustrations with the LSM technique, the Dirac distribution weighted version of the MAPLE implementation was employed, where mean value had six times higher weight than any other point around it. Polynomial approximations of various orders (from the 1^{st} to the 9^{th}) were tested to verify how this order influences probabilistic convergence of the coefficients and moments under consideration. Analogously to the sensitivity gradients they are presented independently with respect to the particle Young's modulus (left series of Figs. 9-20) and – to the matrix modulus – all right graphs in these figures. It is necessary to mention that when one considers randomization of both moduli at the same time it is enough just to add all higher than zeroth perturbation order terms to each other into the probabilistic moments correspondingly and then, recalculate all the coefficients because of the lack of a correlation in-between E_1 and E_2.

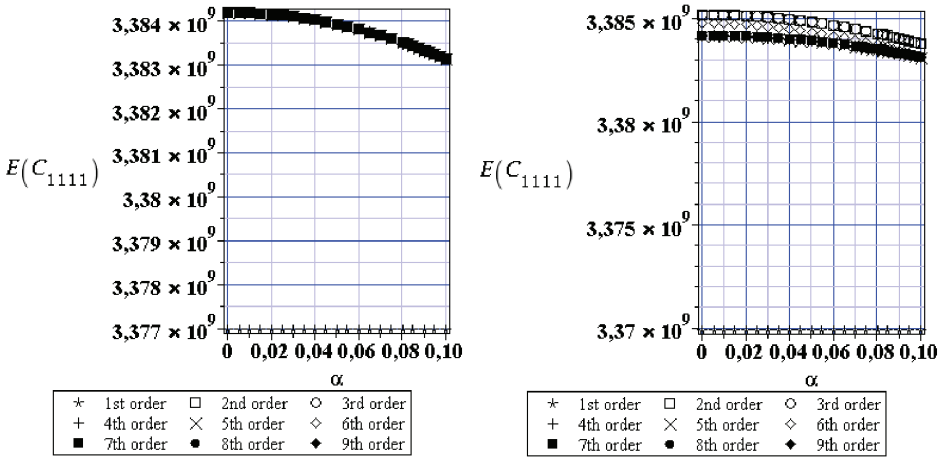

Figure 9: Expected values of $C_{1111}^{(eff)}$ (Pa) with respect to the particle (left) and matrix (right) Young's modulus

Expected values ($E(C_{ijkl}^{(eff)})$) of the effective elasticity tensor are very stable with respect to both random input variables. Although the curves obtained for various polynomial approximations demonstrate high nonlinearity, the vertical axes show

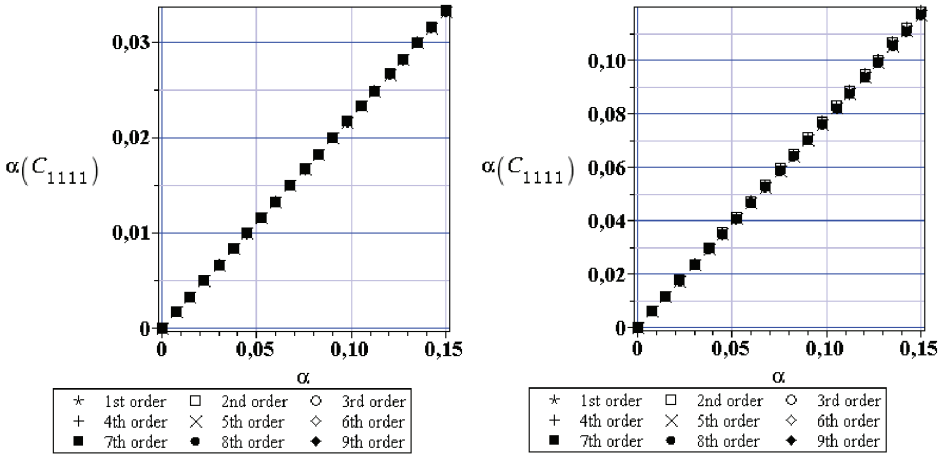

Figure 10: COV of $C_{1111}^{(eff)}$ with respect to the particle (left) and matrix (right) Young's modulus

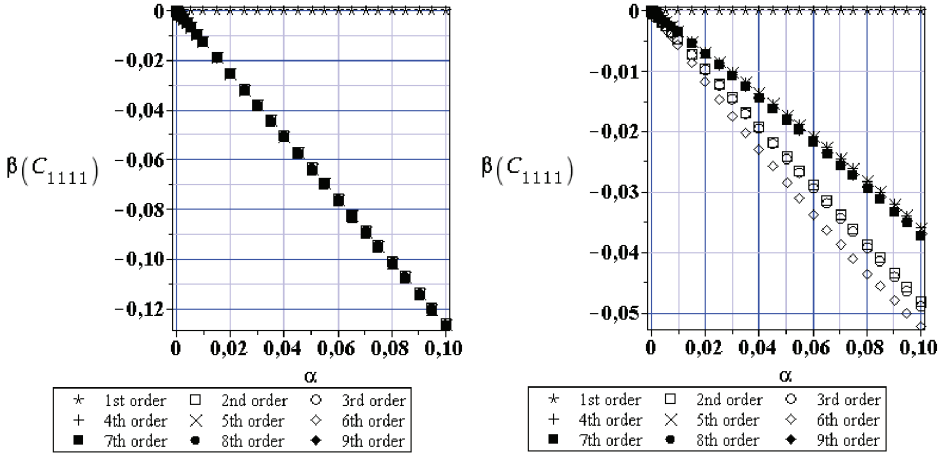

Figure 11: Skewness of $C_{1111}^{(eff)}$ with respect to the particle (left) and matrix (right) Young's modulus

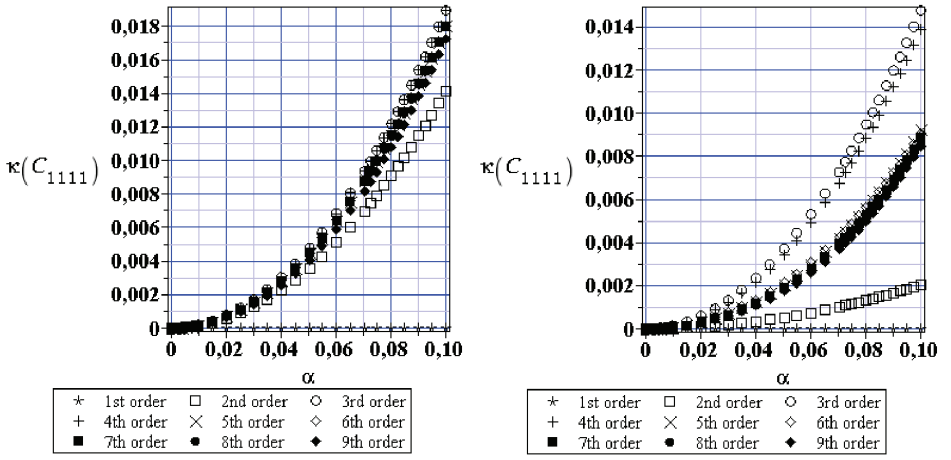

Figure 12: Kurtosis of $C_{1111}^{(eff)}$ with respect to the particle (left) and matrix (right) Young's modulus

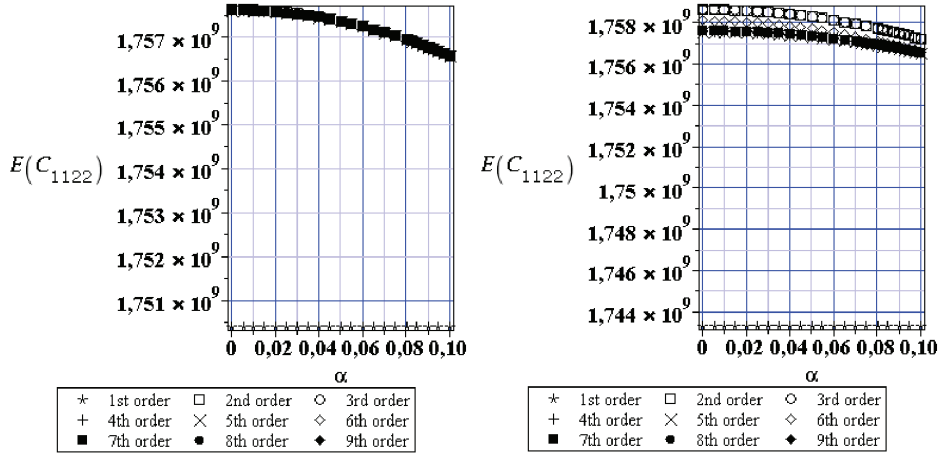

Figure 13: Expected values of $C_{1122}^{(eff)}$ (Pa) with respect to the particle (left) and matrix (right) Young's modulus

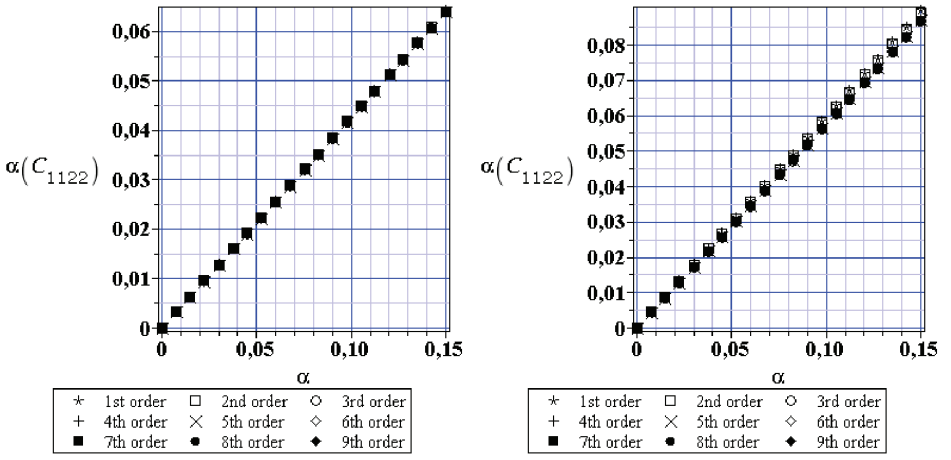

Figure 14: COV of $C_{1122}^{(eff)}$ with respect to the particle (left) and matrix (right) Young's modulus

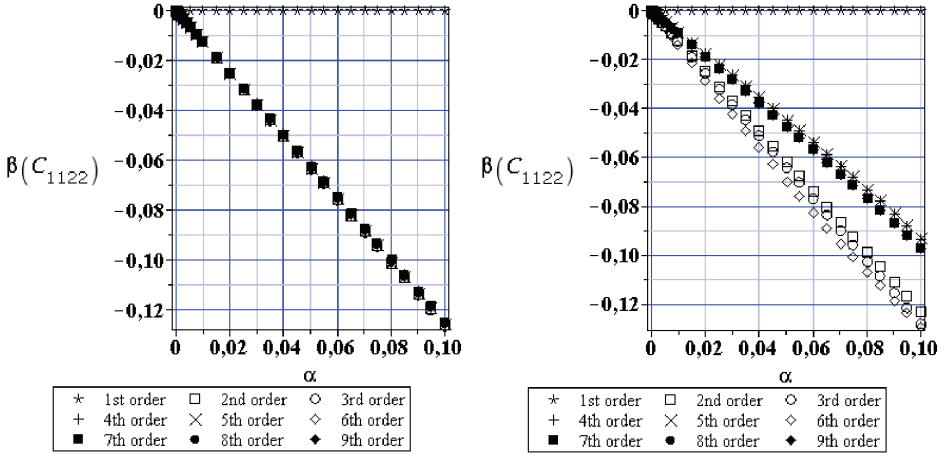

Figure 15: Skewness of $C_{1122}^{(eff)}$ with respect to the particle (left) and matrix (right) Young's modulus

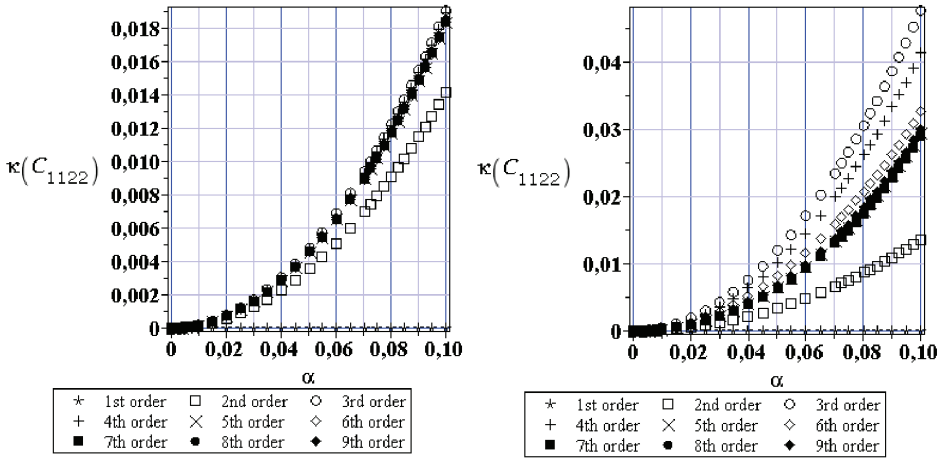

Figure 16: Kurtosis of $C_{1122}^{(eff)}$ with respect to the particle (left) and matrix (right) Young's modulus

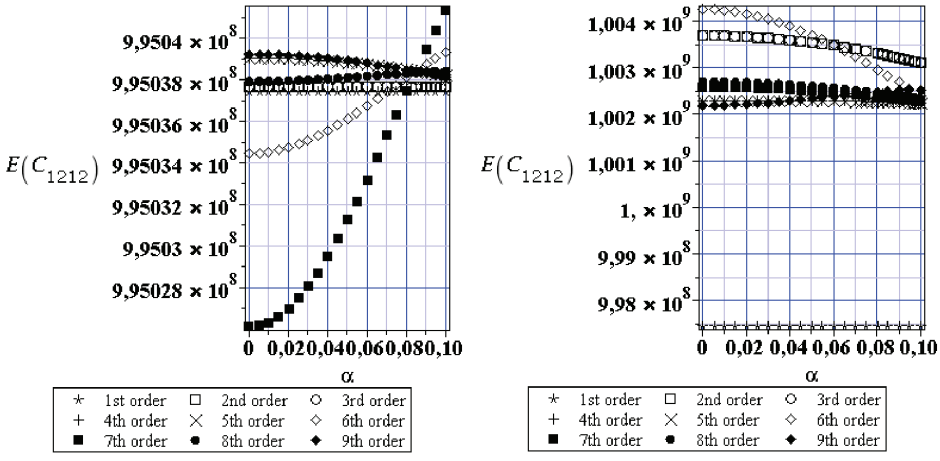

Figure 17: Expected values of $C_{1212}^{(eff)}$ (Pa) with respect to the particle (left) and matrix (right) Young's modulus

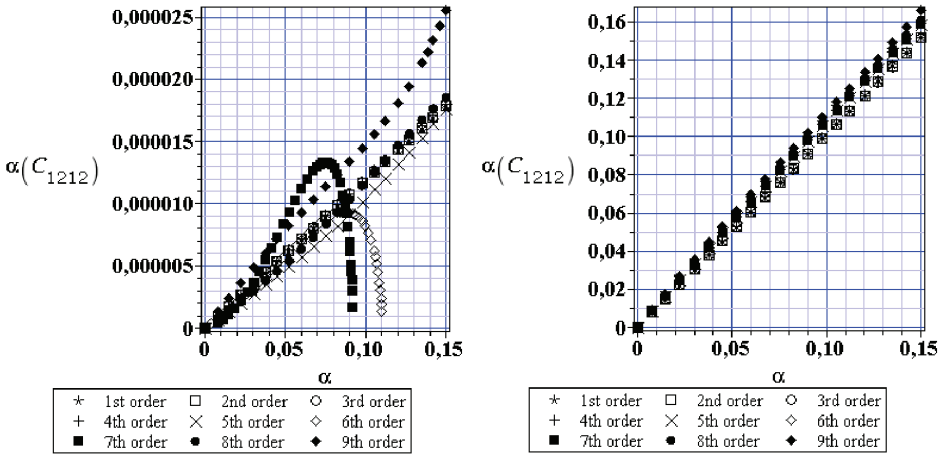

Figure 18: COV of $C_{1212}^{(eff)}$ with respect to the particle (left) and matrix (right) Young's modulus

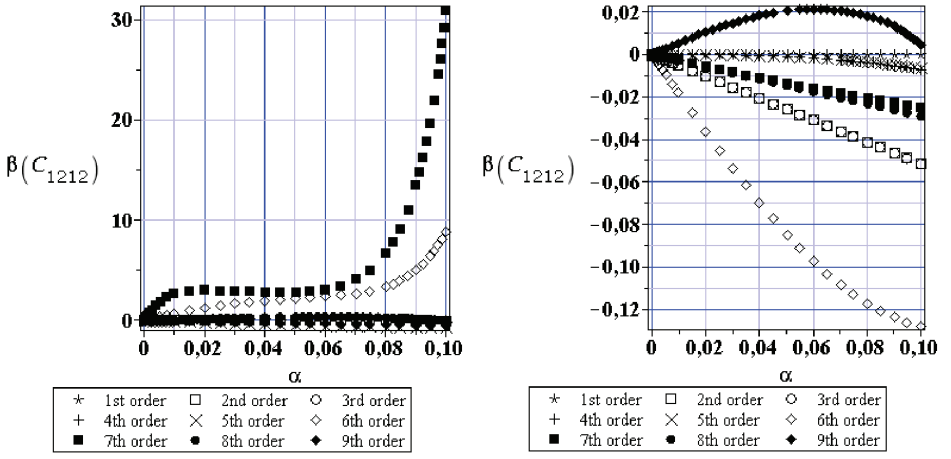

Figure 19: Skewness of $C_{1212}^{(eff)}$ with respect to the particle (left) and matrix (right) Young's modulus

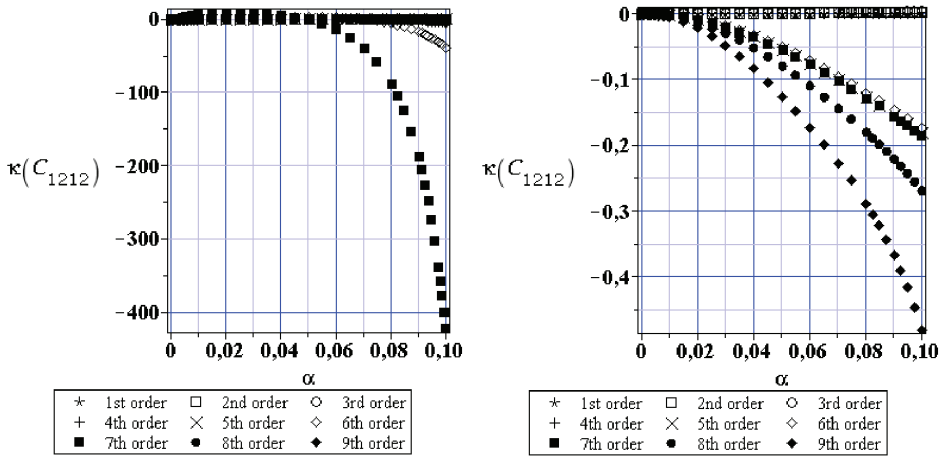

Figure 20: Kurtosis of $C_{1212}^{(eff)}$ with respect to the particle (left) and matrix (right) Young's modulus

that these are quite marginal variations. Practically, they are independent of input coefficient of variation, which is consistent with the Monte-Carlo simulation results in this area [3], and of course expectations in randomization of E_1 and E_2 separately are exactly the same. It is also seen that the lowest orders of an expansion may bring some underestimation for the expectations (see Figs. 9 and 13), while for some intermediate orders one can get some small computational inconsistencies (cf. Fig. 17), resulting from the end oscillatory character of the response functions itself. These expected values usually decrease together with an increasing input coefficient of variation, which may be important for the random inputs having large random deviations (these corresponding to the Young's modulus are most frequently smaller than 0.15). Coefficients of variation (COV) collected in Figs. 10, 14 and 18 show that input polynomial order has practically no influence on their final value, independently of the input coefficient of variation for both input variables; verification of this fact was a motivation to extend computational domain to $\alpha \in [0.0, 0.15]$. Definitely, an uncertainty of the matrix modulus E_2 is more influential on overall randomness of the homogenized tensor, because COVs in this case are more than three times larger for $C_{1111}^{(eff)}$, just only not more than 20% - for $C_{1122}^{(eff)}$. The case of $C_{1212}^{(eff)}$ is very specific as the output COV with respect to E_1 equals almost 0 and significant numerical discrepancies may occur in this extraordinary situation – it means that this component of the effective tensor remains almost deterministic while randomizing Young's modulus of the filler. Further, all

the output coefficients except this specific case are linearly dependent on the input coefficients and, further, are equal to 0 for the lack of any input randomness (a verification of determinism consequence in a structural response).

The behavior of higher order coefficients like skewness in Figs. 11, 15, 19 and kurtosis – cf. Figs. 12, 16 and 20 is essentially more complex as they all depend on input coefficient of variation, approximation order and may be even negative. First observation that can be made is that precise determination of the skewness needs generally higher polynomial order than expectations and coefficients of variation – very stable results with relative error in the range of one percent are obtained here for the largest approximation order. Skewness in all cases starts from 0 (adjacent to the deterministic situation, where α=0) and its absolute value monotonously increases for the first two components of the homogenized tensor with no singularities (at least within the given computational domain), where definitely larger absolute values are obtained during randomization of E_1. Some numerical discrepancies are noticed for $\beta\left(C_{1212}^{(eff)}\right)$ similarly to the moments analyzed before, apparent especially for the 7^{th} (E_1) and the 6^{th} (E_2) order polynomial response function. Independently from the specific component of the homogenized tensor and analysis order, its difference to 0 even for the largest value of the input COV is so small that we can conclude that the output homogenized tensor has almost symmetrical distribution, where the corresponding medians are equal to the expected values. A somewhat different situation is observed for the kurtosis, where a positive and also negative results, depending of course on the response function order, are noticed for the given effective tensor component and the given input random variable.

Generally however, the resulting values of kurtosis are significantly closer to 0 than the skewnesses, so that (taking into account a linear relation of the output versus input coefficients of variation) computed probability distributions of the homogenized tensor have almost the same shape as the bell-shaped Gaussian PDF. Of course, we need to exclude the results obtained for the component $C_{1212}^{(eff)}$, where higher order analyses present mostly numerical discrepancies (in the view of the linear response functions to both E_1 and E_2) and it also confirms this conclusion. The perturbation-based formulas start here from a product of the fourth central probabilistic moment and first as well as second order partial derivatives of the homogenized tensor, so that lower order approximations may accidentally equal 0 for any input coefficient of variation α. If such a lower order response function can be predicted from an analytical model similar to that implemented in the FEM procedure or it follows our engineering modeling experience, we can really postpone higher orders easily. Probabilistic convergence of both skewness and kurtosis for the first two components of the homogenized tensor is very regular in the sense that each new order brings smaller contribution to the overall results, so that 8^{th} or 9^{th}

order approximations practically show no real differences here for any input coefficient α. Nevertheless, all numerical probabilistic results attached collected together show that the resulting effective tensor components have Gaussian distributions as for other composites while randomizing Young's moduli of the components, so that they may be uniquely determined with good accuracy using only their first two probabilistic characteristics. It is necessary to mention that this situation may change a little bit for larger input random fluctuations of the specified variables or significantly - just in case of other randomness' sources during homogenization procedure.

4 Concluding remarks

(1) Computational analysis presented above confirms that the generalized stochastic perturbation technique based on the Weighted Least Squares Method is really very efficient tool for a common determination of the sensitivity gradients and probabilistic moments of the homogenized elasticity tensor, also for rubber-filled polymers. The very detailed sensitivity analysis has shown that the gradients under consideration do not depend on the polynomial response function order and are accurate even for lower order approximations (except linear approximation); the same conclusion may be drawn for the expected values and coefficients of variation in case of the homogenization with an uncertainty in both Young's moduli of the composite constituents. Skewness and kurtosis for the homogenized tensor depend both on the response function order and both input coefficients of variation. However their combination for various input parameters in this study show that the homogenization process preserves Gaussian distribution from input to the output random variables.

(2) Computational study presented in this paper gives also the answer to the key issue in the Stochastic perturbation-based Finite Element Method based on the Response Function Method [Kamiński (2013)] – how to determine the order of the approximating polynomial. We suggest to minimize this order as much as possible to preserve good fitting into the set of trials points taken from the several FEM experiments (not too small) and to avoid any local end oscillations of the resulting function (not too high). Mathematical condition that can be explored further is to minimize the integral of this polynomial calculated numerically or symbolically over a computational domain corresponding to recovery of the response function itself. It can be also done automatically in the symbolic computing environment of such a program like MAPLE.

(3) The stochastic generalized perturbation technique is much faster and more efficient than the Monte-Carlo simulation technique [Cruz and Patera (2011)] in this specific context, where large computational efforts are obviously necessary to de-

termine higher order statistics. Further, it means that all higher probabilistic moments may be derived analytically from the first two for this tensor, where the stochastic perturbation technique appeared to be many times very accurate. Further computational studies in the area of homogenization of rubber-filled polymers may focus on 3D analysis with larger Representative Volume Elements, on higher order homogenization techniques [Fish and Chen (2001)] application, on other types of composites [Fu et al. (2009)] as well as on more realistic nonlinear constitutive models [Gehant et al. (2003); Miehe et al. (2011)].

Acknowledgments

The paper has been written during the visiting professor stay of the first author at *Leibniz-Institut für Polymerforschung Dresden*, *e.V.*, Germany in the period of July-October 2012 and 2013.

References

Bensoussan, A.; Lions, J. L.; Papanicolaou, G. (1978): *Asymptotic Analysis for Periodic Structures*. North-Holland, Amsterdam.

Christensen, R. M. (1979): *Mechanics of Composite Materials*. Wiley, New York.

Cruz, M. E.; Patera, A. T. (1995): A parallel Monte-Carlo finite element procedure for the analysis of multicomponent media. *Int. J. Num. Meth. Engrg.*, vol. 38, pp. 1087-1121.

Dong, L.; Atluri, S. N. (2012): T-Trefftz Voronoi cell finite elements with elastic/rigid inclusions or voids for micromechanical analysis of composite and porous materials. *CMES: Computer Modeling in Engineering and Sciences*, vol. 83, no. 2, pp. 183-219.

Fish, J.; Chen, W. (2001): Higher order homogenization of initial boundary value problem. *J. Engrg. Mech.*, vol. 127, no. 12, pp. 1223–1230.

Fu, S. Y.; Lauke, B.; Mai, Y. W. (2009): *Science and Engineering of Short Fibre Reinforced Polymers*. CRC Press, Boca Raton.

Gehant, S.; Fond, Ch.; Schirrer, R. (2003): Criteria for cavitation of rubber particles: Influence of plastic yielding in the matrix. *Int. J. Fracture*, vol. 122, pp. 161-175.

Jeulin, D.; Ostoja-Starzewski, M., edrs., (2001): *Mechanics of Random and Multiscale Structures*, CISM Courses and Lectures No. 430, Springer, Wien New York.

Kamiński, M. (2005): *Computational Mechanics of Composite Materials*, Springer, London New York.

Kamiński, M. (2009): Sensitivity and randomness in homogenization of periodic fiber-reinforced composites via the response function method. *Int. J. Sol. & Struct.*, vol. 46, no. 3-4, pp. 923–937.

Kamiński, M. (2013): *The Stochastic Perturbation Method for Computational Mechanics*, Wiley, Chichester.

Kamiński, M.; Lauke, B. (2012): Probabilistic and stochastic analysis of the effective properties for the particle reinforced elastomers. *Comput. Mat. Sci.*, vol. 56, pp. 147-160.

Ma, J.; Temizer, I.; Wriggers, P. (2011): Random homogenization analysis in linear elasticity based on analytical bounds and estimates. *Int. J. Sol. Struct*., vol. 48, no. 2, pp. 280-291.

Miehe, Ch.; Diez, J. M.; Goktepe, S.; Schanzel, L. M. (2011) Coupled thermoviscoelastoplasticity of glassy polymers in the logarithmic strain space based on the free volume theory. *Int. J. Sol. Struct*., vol. 48, no. 13, pp. 1799-1817.

Milton, G. W. (2002): *The Theory of Composites*. Cambridge University Press.

Sanchez-Palencia, E. (1980): *Non-Homogeneous Media and Vibration Theory*. Springer-Verlag.

Appendix

The variance of the effective elasticity tensor is derived from a definition and the 10^{th} order stochastic perturbation technique (with the RHS summation over p=1,...,M) as

$$
\begin{aligned}
&Var\left(C_{ijkl}^{(eff)}\right) = \mu_2\left(C_{ijkl}^{(eff)}\right) = \int_{-\infty}^{+\infty}\left(C_{ijkl}^{(eff)} - E\left[C_{ijkl}^{(eff)}\right]\right)^2 g(b_p)\,db_p \\
&= \sum_{p=1}^{n}\mu_2(b_p)\left(\frac{\partial C_{ijkl}^{(eff)}}{\partial b_p}\right)^2 + \sum_{p=1}^{n}\mu_4(b_p)\left\{\frac{1}{4}\left(\frac{\partial^2 C_{ijkl}^{(eff)}}{\partial b_p^2}\right)^2 + \frac{1}{3}\frac{\partial^3 C_{ijkl}^{(eff)}}{\partial b_p^3}\frac{\partial C_{ijkl}^{(eff)}}{\partial b_p}\right\} \\
&+ \sum_{p=1}^{n}\mu_6(b_p)\left\{\frac{1}{36}\left(\frac{\partial^3 C_{ijkl}^{(eff)}}{\partial b_p^3}\right)^2 + \frac{1}{24}\frac{\partial^4 C_{ijkl}^{(eff)}}{\partial b_p^4}\frac{\partial^2 C_{ijkl}^{(eff)}}{\partial b_p^2} + \frac{1}{60}\frac{\partial^5 C_{ijkl}^{(eff)}}{\partial b_p^5}\frac{\partial C_{ijkl}^{(eff)}}{\partial b_p}\right\} \\
&+ \sum_{p=1}^{n}\mu_8(b_p)\left\{\frac{1}{2520}\frac{\partial^7 C_{ijkl}^{(eff)}}{\partial b_p^7}\frac{\partial C_{ijkl}^{(eff)}}{\partial b_p} + \frac{1}{720}\frac{\partial^6 C_{ijkl}^{(eff)}}{\partial b_p^6}\frac{\partial^2 C_{ijkl}^{(eff)}}{\partial b_p^2}\right\} \\
&+ \sum_{p=1}^{n}\mu_8(b_p)\left\{\frac{1}{576}\left(\frac{\partial^4 C_{ijkl}^{(eff)}}{\partial b_p^4}\right)^2 + \frac{1}{360}\frac{\partial^5 C_{ijkl}^{(eff)}}{\partial b_p^5}\frac{\partial^3 C_{ijkl}^{(eff)}}{\partial b_p^3}\right\} \\
&+ \sum_{p=1}^{n}\mu_{10}(b_p)\left\{\frac{1}{14400}\left(\frac{\partial^5 C_{ijkl}^{(eff)}}{\partial {b_p}^5}\right)^2 + \frac{1}{40320}\frac{\partial^8 C_{ijkl}^{(eff)}}{\partial {b_p}^8}\frac{\partial^2 C_{ijkl}^{(eff)}}{\partial {b_p}^2}\right. \\
&\left.+ \frac{1}{8640}\frac{\partial^6 C_{ijkl}^{(eff)}}{\partial {b_p}^6}\frac{\partial^4 C_{ijkl}^{(eff)}}{\partial {b_p}^4}\right\} \\
&+ \sum_{p=1}^{n}\mu_{10}(b_p)\left\{\frac{1}{15120}\frac{\partial^7 C_{ijkl}^{(eff)}}{\partial b_p^7}\frac{\partial^3 C_{ijkl}^{(eff)}}{\partial b_p^3} + \frac{1}{181440}\frac{\partial^9 C_{ijkl}^{(eff)}}{\partial b_p^9}\frac{\partial C_{ijkl}^{(eff)}}{\partial b_p}\right\}
\end{aligned}
\tag{A1}
$$

The additional perturbation – based third central probabilistic moment of this tensor is derived as (with analogous summation over independent p=1,...,M contributions)

$$\mu_3\left(C_{ijkl}^{(eff)}\right)=\int_{-\infty}^{+\infty}\left(C_{ijkl}^{(eff)}-E\left[C_{ijkl}^{(eff)}\right]\right)^3 p\left(b_p\right)db_p$$

$$=\int_{-\infty}^{+\infty}\left(C_{ijkl}^{(eff)^0}+\varepsilon\frac{\partial C_{ijkl}^{(eff)}}{\partial b_p}\Delta b+\ldots-E\left[C_{ijkl}^{(eff)}\right]\right)^3 g\left(b_p\right)db_p\cong$$

$$+\varepsilon^4\mu_4\left(b_p\right)\left(\frac{3}{2}\left(\frac{\partial C_{ijkl}^{(eff)}}{\partial b_p}\right)^2\frac{\partial^2 C_{ijkl}^{(eff)}}{\partial b_p^2}\right)$$

$$+\varepsilon^6\mu_6(b_p)\left(\frac{1}{2}\frac{\partial C_{ijkl}^{(eff)}}{\partial b_p}\frac{\partial^2 C_{ijkl}^{(eff)}}{\partial b_p^2}\frac{\partial^3 C_{ijkl}^{(eff)}}{\partial b_p^3}+\frac{1}{8}\left(\frac{\partial C_{ijkl}^{(eff)}}{\partial b_p}\right)^2\frac{\partial^4 C_{ijkl}^{(eff)}}{\partial b_p^4}+\frac{1}{8}\left(\frac{\partial^2 C_{ijkl}^{(eff)}}{\partial b_p^2}\right)^3\right)$$

$$+\varepsilon^8\mu_8\left(b_p\right)\left(\frac{1}{240}\left(\frac{\partial C_{ijkl}^{(eff)}}{\partial b_p}\right)^2\frac{\partial^6 C_{ijkl}^{(eff)}}{\partial b_p^6}+\frac{1}{24}\left(\frac{\partial^3 C_{ijkl}^{(eff)}}{\partial b_p^3}\right)^2\frac{\partial^2 C_{ijkl}^{(eff)}}{\partial b_p^2}\right.$$

$$\left.+\frac{1}{32}\left(\frac{\partial^2 C_{ijkl}^{(eff)}}{\partial b_p^2}\right)^2\frac{\partial^4 C_{ijkl}^{(eff)}}{\partial b_p^4}\right)$$

$$+\varepsilon^8\mu_8\left(b_p\right)\left(\frac{1}{40}\frac{\partial C_{ijkl}^{(eff)}}{\partial b_p}\frac{\partial^2 C_{ijkl}^{(eff)}}{\partial b_p^2}\frac{\partial^5 C_{ijkl}^{(eff)}}{\partial b_p^5}+\frac{1}{24}\frac{\partial C_{ijkl}^{(eff)}}{\partial b_p}\frac{\partial^3 C_{ijkl}^{(eff)}}{\partial b_p^3}\frac{\partial^4 C_{ijkl}^{(eff)}}{\partial b_p^4}\right)$$

$$+\varepsilon^{10}\mu_{10}\left(b_p\right)\left(+\frac{1}{1680}\frac{\partial C_{ijkl}^{(eff)}}{\partial b_p}\frac{\partial^2 C_{ijkl}^{(eff)}}{\partial b_p^2}\frac{\partial^7 C_{ijkl}^{(eff)}}{\partial b_p^7}\right.$$

$$\left.+\frac{1}{720}\frac{\partial C_{ijkl}^{(eff)}}{\partial b_p}\frac{\partial^3 C_{ijkl}^{(eff)}}{\partial b_p^3}\frac{\partial^6 C_{ijkl}^{(eff)}}{\partial b_p^6}+\frac{1}{480}\frac{\partial C_{ijkl}^{(eff)}}{\partial b_p}\frac{\partial^4 C_{ijkl}^{(eff)}}{\partial b_p^4}\frac{\partial^5 C_{ijkl}^{(eff)}}{\partial b_p^5}\right)$$

$$+\varepsilon^{10}\mu_{10}\left(b_p\right)\left(\frac{1}{240}\frac{\partial^2 C_{ijkl}^{(eff)}}{\partial b_p^2}\frac{\partial^3 C_{ijkl}^{(eff)}}{\partial b_p^3}\frac{\partial^5 C_{ijkl}^{(eff)}}{\partial b_p^5}+\frac{1}{13440}\left(\frac{\partial C_{ijkl}^{(eff)}}{\partial b_p}\right)^2\frac{\partial^8 C_{ijkl}^{(eff)}}{\partial b_p^8}\right)$$

(A2)

$$
\begin{aligned}
\mu_4\left(C_{ijkl}^{(eff)}\right) &= \varepsilon^4\mu_4\left(b_p\right)\left(\frac{\partial C_{ijkl}^{(eff)}}{\partial b_p}\right)^4 \\
&+\varepsilon^6\mu_6\left(b_p\right)\left(\frac{2}{3}\left(\frac{\partial C_{ijkl}^{(eff)}}{\partial b_p}\right)^3\frac{\partial^3 C_{ijkl}^{(eff)}}{\partial b_p^3}+\frac{3}{2}\left(\frac{\partial C_{ijkl}^{(eff)}}{\partial b_p}\right)^2\left(\frac{\partial^2 C_{ijkl}^{(eff)}}{\partial b_p^2}\right)^2\right) \\
&+\varepsilon^8\mu_8\left(b_p\right)\left(\frac{1}{16}\left(\frac{\partial^2 C_{ijkl}^{(eff)}}{\partial b_p^2}\right)^4+\frac{1}{4}\left(\frac{\partial C_{ijkl}^{(eff)}}{\partial b_p}\right)^2\frac{\partial^2 C_{ijkl}^{(eff)}}{\partial b_p^2}\frac{\partial^4 C_{ijkl}^{(eff)}}{\partial b_p^4}\right. \\
&\left.+\frac{1}{30}\left(\frac{\partial C_{ijkl}^{(eff)}}{\partial b_p}\right)^3\frac{\partial^5 C_{ijkl}^{(eff)}}{\partial b_p^5}\right) \\
&+\varepsilon^8\mu_8\left(b_p\right)\left(\frac{1}{6}\left(\frac{\partial C_{ijkl}^{(eff)}}{\partial b_p}\right)^2\left(\frac{\partial^3 C_{ijkl}^{(eff)}}{\partial b_p^3}\right)^2+\frac{1}{2}\frac{\partial C_{ijkl}^{(eff)}}{\partial b_p}\left(\frac{\partial^2 C_{ijkl}^{(eff)}}{\partial b_p^2}\right)^2\frac{\partial^3 C_{ijkl}^{(eff)}}{\partial b_p^3}\right) \\
&+\varepsilon^{10}\mu_{10}\left(b_p\right)\left(\frac{1}{1260}\left(\frac{\partial C_{ijkl}^{(eff)}}{\partial b_p}\right)^3\frac{\partial^7 C_{ijkl}^{(eff)}}{\partial b_p^7}\right. \\
&+\frac{1}{120}\left(\frac{\partial C_{ijkl}^{(eff)}}{\partial b_p}\right)^2\frac{\partial^2 C_{ijkl}^{(eff)}}{\partial b_p^2}\frac{\partial^6 C_{ijkl}^{(eff)}}{\partial b_p^6}+\frac{1}{96}\left(\frac{\partial C_{ijkl}^{(eff)}}{\partial b_p}\right)^2\left(\frac{\partial^4 C_{ijkl}^{(eff)}}{\partial b_p^4}\right)^2\Bigg) \\
&+\varepsilon^{10}\mu_{10}\left(b_p\right)\left(\frac{1}{54}\frac{\partial C_{ijkl}^{(eff)}}{\partial b_p}\left(\frac{\partial^3 C_{ijkl}^{(eff)}}{\partial b_p^3}\right)^3\right. \\
&+\frac{1}{48}\left(\frac{\partial^2 C_{ijkl}^{(eff)}}{\partial b_p^2}\right)^3\frac{\partial^4 C_{ijkl}^{(eff)}}{\partial b_p^4}+\frac{1}{24}\left(\frac{\partial^2 C_{ijkl}^{(eff)}}{\partial b_p^2}\right)^2\left(\frac{\partial^3 C_{ijkl}^{(eff)}}{\partial b_p^3}\right)^2\Bigg) \\
&+\varepsilon^{10}\mu_{10}\left(b_p\right)\left(\frac{1}{40}\frac{\partial C_{ijkl}^{(eff)}}{\partial b_p}\left(\frac{\partial^2 C_{ijkl}^{(eff)}}{\partial b_p^2}\right)^2\frac{\partial^5 C_{ijkl}^{(eff)}}{\partial b_p^5}+\frac{1}{60}\left(\frac{\partial C_{ijkl}^{(eff)}}{\partial b_p}\right)^2\frac{\partial^3 C_{ijkl}^{(eff)}}{\partial b_p^3}\frac{\partial^5 C_{ijkl}^{(eff)}}{\partial b_p^5}\right. \\
&\left.+\frac{1}{12}\frac{\partial^2 C_{ijkl}^{(eff)}}{\partial b_p^2}\frac{\partial C_{ijkl}^{(eff)}}{\partial b_p}\frac{\partial^3 C_{ijkl}^{(eff)}}{\partial b_p^3}\frac{\partial^4 C_{ijkl}^{(eff)}}{\partial b_p^4}\right)
\end{aligned}
\tag{A3}
$$